An azumamide C analogue without the zinc-binding functionality

Villadsen, Jesper; Kitir, Betül; Wich, Kathrine; Friis, Tina; Madsen, Andreas Stahl; Olsen, Christian Adam

Published in:
MedChemComm

Link to article, DOI:
10.1039/C4MD00252K

Publication date:
2014

Document Version
Publisher's PDF, also known as Version of record

MedChemComm

CONCISE ARTICLE

View Article Online
View Journal

Cite this: DOI: 10.1039/c4md00252k

An azumamide C analogue without the zinc-binding functionality†

Jesper S. Villadsen,[a] Betül Kitir,‡[a] Kathrine Wich,‡ Tina Friis,[b] Andreas S. Madsen‡[a] and Christian A. Olsen‡*[a]

Histone deacetylase (HDAC) inhibitors have attracted considerable attention due to their promise as therapeutic agents. Most HDAC inhibitors adhere to a general "cap-linker-Zn^{2+}-binding group" architecture but recent studies have indicated that potent inhibition may be achieved without a Zn^{2+}-coordinating moiety. Herein, we describe the synthesis of an azumamide analogue lacking its native Zn^{2+}-binding group and evaluation of its inhibitory activity against recombinant human HDAC1–11. Furthermore, kinetic investigation of the inhibitory mechanism of both parent natural product and synthetic analogue against HDAC3-NCoR2 is reported as well as their activity against Burkitt's lymphoma cell proliferation.

Received 13th June 2014
Accepted 11th August 2014

DOI: 10.1039/c4md00252k

www.rsc.org/medchemcomm

Introduction

Histone deacetylase (HDAC) enzymes,[1,2] or perhaps more appropriately termed lysine deacylases (KDACs),[3–5] have attracted attention as putative therapeutic targets,[6–9] especially due to their ability to modify the landscape of post-translational modifications (PTMs) on histone proteins in chromatin.[6] Indeed, two HDAC inhibitors [*i.e.*, SAHA (vorinostat, marketed as Zolinza®)[10] and romidepsin (FK228, marketed as Istodax®)[11]] have received approval by the Food and Drug Administration in the US for treatment of cutaneous T-cell lymphoma, and several other compounds are currently in clinical trials for additional indications.[12]

In addition to the depsipeptide romidepsin mentioned above, Nature has provided a variety of potent macrocyclic HDAC inhibitors such as the trapoxins, apicidins, azumamides, chlamydocin, and largazole.[13–15] The apicidin structure (**1**)[16] has been the subject of numerous structure–activity relationship studies,[17–23] and recently, analogues without the so-called Zn^{2+}-binding group (the ethylketone moiety) were investigated by Ghadiri and coworkers (*e.g.*, **2** and **3**, Scheme 1).[24] The Zn^{2+}-binding side chain was substituted with various alkyl groups, and the optimal side chain at this position was a non-branched propyl group. Not surprisingly, these inhibitors were significantly less potent than their ethylketone-containing counterparts, but still exhibited K_i-values of just 30–50 nM against HDACs 1–3.[24] Since a wide variety of enzymes rely on metal ions for catalytic activity, excision of the Zn^{2+}-binding group may enable development of more selective HDAC inhibitors with fewer adverse effects.

We found this idea attractive and decided to investigate the macrocyclic core of the azumamides[25–27] (**4–8**) in a similar fashion by synthesizing compound **9** (Scheme 1). The azumamides contain relatively weak Zn^{2+}-binding groups (carboxylate or carboxyamide)[28] while still exhibiting high potency as class I HDAC inhibitors with low nanomolar K_i-values recorded for

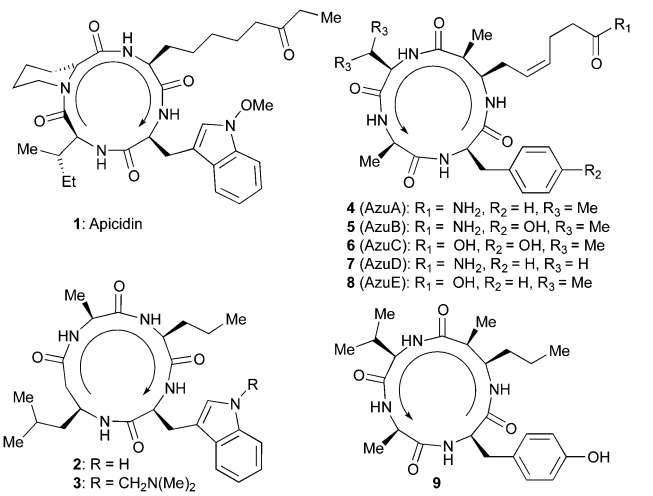

Scheme 1 Structures of cyclic peptide HDAC inhibitors. Arrows show the opposite N → C directionality of apicidin and azumamide.

[a]Department of Chemistry, Technical University of Denmark, Kemitorvet 207, Kongens Lyngby, DK-2800, Denmark. E-mail: cao@sund.ku.dk; Tel: +45 45252105

[b]Department of Clinical Biochemistry, Immunology and Genetics (KBIG), Statens Serum Institut, Artillerivej 5, DK-2300, Copenhagen, Denmark

† Electronic supplementary information (ESI) available: Materials and methods, supplementary tables and figures, as well as ^1H and ^{13}C NMR spectra of the prepared compounds. See DOI: 10.1039/c4md00252k

‡ Present address: Center for Biopharmaceuticals and Department of Drug Design and Pharmacology, University of Copenhagen, Universitetsparken 2, DK-2100, Copenhagen, Denmark.

azumamides C (**6**) and E (**8**).[29] Since azumamide C was slightly more potent than azumamide E, we substituted the Zn^{2+}-binding side chain of the β-amino acid in compound **6** with a propyl group to give compound **9**. In addition to removal of the metal-coordinating capability, removal of this negatively charged carboxylate, may furthermore improve cell permeability of the ligand. We here present the synthesis and evaluation of compound **9** as an HDAC inhibitor.

Results and discussion

Chemistry

The three D-amino acids necessary to prepare compound **9** were purchased and the β-amino acid building block (**14**, Scheme 2) was prepared using chiral sulfinylimine **12**, which was obtained by condensation of butanal (**10**) and (*S*)-2-methylpropane-2-sulfinamide ("Ellman's auxiliary", **11**).[30,31] The diastereoselective Mannich reaction between imine (**12**) and the *Z*-enolate of *tert*-butyl propionate provided the (2*S*,3*R*)-β-amino ester (**13**) as the major diastereoisomer. Acid mediated cleavage of the *tert*-butyl ester and the sulfinyl group with both TFA and HCl to ensure full conversion, afforded the fully deprotected β-amino acid and subsequent treatment with Fmoc-OSu furnished the desired β-amino acid building block (**14**).

Unfortunately, we were unable to obtain crystals for determination of the absolute stereochemistry by X-ray crystallography. Thus, the stereochemistry was instead confirmed by conversion of sulfinyl-protected *tert*-butyl ester **13** to the previously reported Cbz-protected methyl ester (**15**, Scheme 3) and both optical rotation and NMR data were in full agreement with the previously reported data[32] (see also ESI, Table S1†).

Coupling of the β-amino acid (**14**) to a resin-bound tripeptide [H–D-Val–D-Ala–D-Tyr–(2-chlorotrityl-resin)] using HATU, followed by removal of the Fmoc group and cleavage from the resin afforded linear tetrapeptide **16**. Macrolactamization, under dilute conditions (0.4 mM in DMF), using HATU as the coupling reagent afforded target peptide **9** (Scheme 4). The relatively low yield is similar to those previously achieved for similar compounds[21–24] and may, at least in part, be attributed to poor solubility in the water–acetonitrile mobile phase used in reversed-phase HPLC purification. However, further optimization of cyclization efficiency, which is known to be notoriously troublesome for small peptides,[33] may also prove worthwhile.

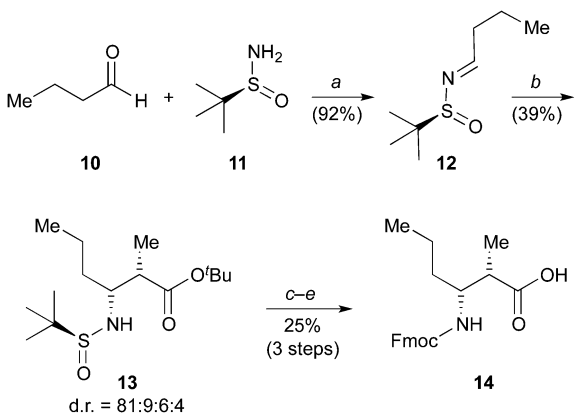

Scheme 2 Reagents and conditions: (a) $CuSO_4$ (5.0 equiv.), anhydrous CH_2Cl_2, rt, 20 h; (b) *tert*-butyl propionate (2.5 equiv.), LDA (2.6 equiv.), HMPA (5.7 equiv.), anhydrous THF, −78 °C, 30 min; then imine **12**; (c) TFA–CH_2Cl_2 (1 : 1), rt, 5 h; (d) HCl (4.0 M in dioxane, 3.0 equiv.), dioxane, rt, 1.5 h; (e) Na_2CO_3 (4.0 equiv.), Fmoc-OSu (1.2 equiv.), DMF–H_2O, 0 °C → rt, 3 h.

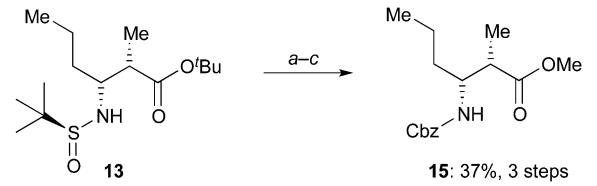

Scheme 3 Reagents and conditions: (a) HCl (4M in dioxane, 30 equiv.), MeOH, rt, 22 h; (b) thionyl chloride (3.0 equiv.), MeOH, 0 °C → reflux, 23 h, then thionyl chloride (1.5 equiv.), MeOH, 0 °C → rt, 22 h; (c) EtOAc, saturated aqueous $NaHCO_3$, benzylchloroformate, rt, 18 h.

Profiling of HDAC inhibitory activity

We first screened the new compound along with a non-cyclized azumamide C analogue (for structure, see ESI, Fig. S1†), and SAHA as internal control against the full panel of recombinant human HDACs 1–11 applying a single inhibitor concentration (ESI, Fig. S1†). The linear peptide was included to address the importance of the macrocyclic nature of the azumamides and, somewhat expectedly, the linear compound was not inhibiting any of the HDACs potently. Poor inhibitory activities were also observed for macrocycle **9** against class I HDAC8, class IIa HDACs (4, 5, 7, and 9), and class IIb HDAC6, and it was therefore decided to proceed with full dose–response profiling only against HDACs 1–3, 10, and 11 (ESI, Fig. S2†).

To be able to compare potencies irrespective of applied substrate identity and concentration in the assays, we determined K_i-values using the Cheng–Prusoff equation[34] and the K_m-values for the selected substrate–enzyme combinations (Table 1).[29,35,36] Not surprisingly, compound **9** was less potent than its parent compound, azumamide C.

Still, compound **9** exhibited low micromolar inhibition of class I HDACs even without the ability to coordinate to Zn^{2+} in the active site. Interestingly, the edited analogue (**9**) was either equipotent or slightly more potent than the corresponding carboxamide-containing natural product azumamide B (Table 1 and ESI, Fig. S2†). The azumamide core, however, could not compete with the most potent compounds from the more elaborate series

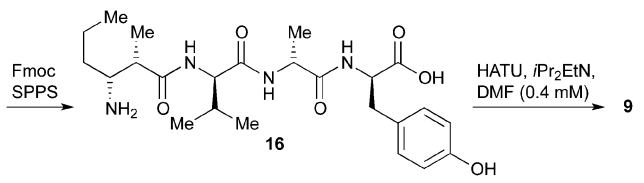

Scheme 4 Macrolactamization to give compound **9** (7%, based on resin loading).

Table 1 K_i-values (μM) against HDAC isoforms from different classes[a]

	Class I			Class II	Class IV
Compd	HDAC1	HDAC2	HDAC3[b]	HDAC10	HDAC11
9	2.4 ± 0.8	1.4 ± 0.7	3.0 ± 0.1	4 ± 1	6 ± 1
AzuB (**5**)	5[c]	3[c]	3[c]	—	>5[c]
AzuC (**6**)	0.02 ± 0.01	0.01 ± 0.006	0.018 ± 0.001	0.02 ± 0.005	0.06 ± 0.008
SAHA	0.01 ± 0.006	0.008 ± 0.004	0.022 ± 0.001	0.04 ± 0.02	0.06 ± 0.02

[a] Values were calculated from at least two individual dose–response experiments performed in duplicate using the Cheng–Prusoff equation. [b] Recombinant human HDAC3 was purchased as a complex with the deacetylase-activating domain of nuclear receptor co-repressor 2 (NCoR2). [c] From a previous publication.[29]

of cyclotetrapeptide HDAC inhibitors without Zn^{2+}-binding groups previously reported.[24]

Kinetic evaluation of HDACi activity

Since compound **9** was relatively potent against HDAC3 and since HDAC3 was the only enzyme in complex with its co-repressor,[37] which may affect the inhibitor potency,[38] we chose to investigate this interaction in more detail by kinetic experiments. Performing progression curve inhibition experiments where the enzymatic catalysis is followed over time in the presence of various inhibitor concentrations may reveal insights regarding the mechanism of inhibition. A recent study demonstrated a slow-binding mechanism of benzamide-based inhibitors against HDAC3-NCoR2,[39] that would not be revealed by simple dose–response experiments performed in an endpoint fashion. We thus performed similar experiments to investigate the mechanism of inhibition exhibited by both azumamide C (**6**) and compound **9**, with SAHA included as a control compound (Fig. 1).

In all cases, the linear progression curves revealed a constant rate of substrate conversion over time, which indicate a standard fast-on–fast-off mechanism of inhibition. This is in agreement with previous findings for SAHA[39] and non-Zn^{2+}-binding macrocycles,[24] but to the best of our knowledge, this is the first investigation of the mechanism of inhibition by azumamide natural products.

The K_i-values derived from fitting the continuous assay data were generally 2–4-fold lower than those obtained by applying the Cheng–Prusoff equation to simple dose–response results (Table 1). The respective values were in the same range, however, and the relationship between compound potencies showed the same trend. Thus, we find the dose–response/Cheng–Prusoff method to be sufficient for determination of K_i-values of compounds with a known fast-on–fast-off inhibition mechanism.

Effect on cultured cancer cells

Epigenetic silencing of the proapototic Bcl-2-family gene, Bim, in Burkitt's lymphoma cells by concurrent promoter hypermethylation and deacetylation has been demonstrated to be involved in the mechanism underlying the common chemoresistance of Burkitt's lymphoma. This chemoresistance has been reversed by treatment with the HDAC inhibitor SAHA.[40] To investigate whether our compounds could influence proliferation of lymphoma cells, we tested their effect on the Epstein Barr virus (EBV)-infected human Burkitt's lymphoma cell line, EB-3.

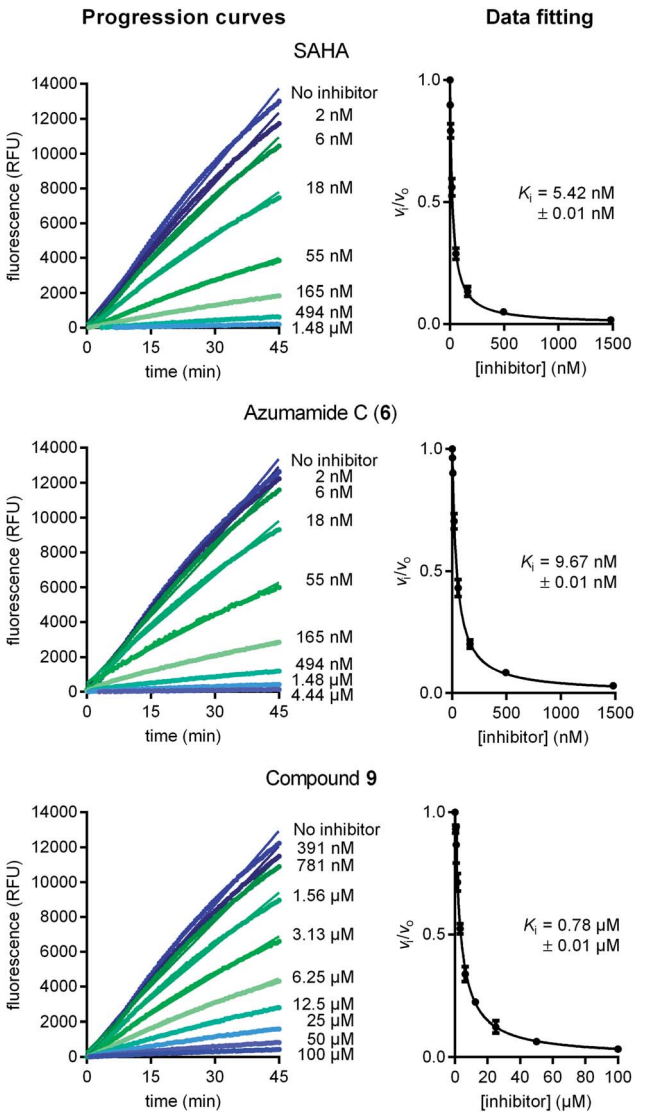

Fig. 1 Progression curves and data fitting of the inhibition of HDAC3-NCoR2. Data were fitted to the equation, $v_i/v_0 = (1 + [I]/(K_i(1 + [S]/K_m)))^{-1}$, using the GraphPad Prism software to derive the K_i-values shown in the figure above.

To assess the effects of azumamides B (**5**) and C (**6**) as well as compound **9** along with positive controls SAHA and apicidin, we used the MTT assay, in which cleavage of yellow MTT affords purple formazan crystals in functioning mitochondria to give a measure of cell viability. Initially, we screened all five compounds in triplicate at 10 μM and only the positive controls, SAHA and apicidin inhibited cell proliferation. We therefore tested the compounds starting at higher concentrations of the macrocycles. Since all compound stock solutions were prepared in DMSO due to solubility issues, we tested 2-fold dilutions of DMSO (from 1%) in parallel with the 2-fold serial dilutions of the compounds. Based on this, SAHA and apicidin exhibited GI_{50} values of 2.8 μM and 0.8 μM, respectively. For apicidin, this correlates well with values previously obtained against HeLa, Hct-116, MCF-7, KYO-1, and K-562 cells.[23] The EB-3 cell proliferation was inhibited at 1% but not at 0.5% DMSO and this resulted in a maximal reliable concentration of azumamide C of 25 μM while it was 50 μM for azumamide B and **9**. For all three compounds the GI_{50} values were deemed well above this limit as no reproducible growth inhibition was observed for any of the compounds.

Conclusions

In the present study, we have synthesized an analogue of the naturally occurring HDAC inhibitor, azumamide C, which is structurally edited to prevent coordination to the zinc ion present in the HDAC enzyme active sites. This allowed us to elucidate the binding affinity of the natural product's macrocyclic core, which proved to be in the low- to sub-micromolar range. We furthermore, showed that both natural product and its analogue inhibit HDAC3-NCoR2 *via* a fast-on–fast-off mechanism by performing continuous assay experiments.

Not surprisingly, this non-Zn^{2+}-binding analogue was significantly less potent than its carboxylate-containing parent compound against HDACs. However, it is quite remarkable that our synthetic analogue was at least as potent as the corresponding carboxamide-containing natural product azumamide B (**5**). It is puzzling that the marine sponge, from where the natural products were originally isolated,[26] produces these carboxamide-containing compounds that seem to adhere to the general pharmacophore for HDAC inhibition, but apparently contain a redundant Zn^{2+}-binding group. We finally tested the compounds' ability to inhibit proliferation of EB-3 cells *in vitro*. Contrary to both SAHA and apicidin none of the tested azumamide analogues were potent growth inhibitors, which underscores that a fine-tuned combination of HDACi potency and cell permeability is required for activity in cells.

Experimental

Synthetic procedures

(*S*,*E*)-*N*-Butylidene-2-methylpropane-2-sulfinamide (12). A solution of butyraldehyde (0.80 mL, 8.91 mmol, 2.0 equiv.) in anhydrous CH_2Cl_2 (1.0 mL) was added dropwise to a solution of anhydrous $CuSO_4$ (3.6 g, 22.6 mmol, 5.0 equiv.) and (*S*)-(−)-2-methyl-2-propanesulfinamide (0.54 g, 4.46 mmol) in anhydrous CH_2Cl_2 (7.0 mL). After stirring vigorously for 20 hours the reaction mixture was filtered through a pad of Celite and the filter cake washed with CH_2Cl_2. The combined organic phases were concentrated *in vacuo* and purification by vacuum silica gel chromatography afforded *tert*-butanesulfinyl imine **12** (0.72 g, 92%) as a colorless oil. ^{1}H NMR (300 MHz, $CDCl_3$) δ 8.03 (t, J = 4.7 Hz, 1H), 2.46 (td, J = 7.3, 4.7 Hz, 2H), 1.63 (h, J = 7.4 Hz, 2H), 1.16 (s, 9H), 0.95 (t, J = 7.4 Hz, 3H); ^{13}C NMR (75 MHz, $CDCl_3$) δ 169.7, 56.5, 38.1, 22.5, 19.0, 13.9. Spectral data were in agreement with previously reported data.[41]

(2*S*,3*R*)-*tert*-Butyl 3-((*S*)-1,1-dimethylethylsulfinamido)-2-methylhexanoate (13). A solution of LDA (1.5 M in THF, 5.0 mL, 7.5 mmol, 2.6 equiv.) was added dropwise over 5 min to a solution of HMPA (1.5 mL, 8.6 mmol, 5.7 equiv.) in dry THF (5.0 mL) at −78 °C. After 15 min, *tert*-butyl propionate (1.1 mL, 7.3 mmol, 2.5 equiv.) was added dropwise and after stirring for additionally 30 min imine **12** (0.51 g, 2.90 mmol) in anhydrous THF (2.0 mL) was added dropwise. After 2 hours the reaction was quenched with sat. aqueous NH_4Cl and warmed to room temperature. Aqueous HCl (1 M, 20 mL) was added and the mixture extracted with EtOAc (2 × 60 mL). The combined organic phases were washed with brine (40 mL), dried ($MgSO_4$), filtered, and concentrated *in vacuo*. Diastereoselectivity was determined by ^{1}H NMR integration of the crude reaction mixture (65 : 25 : 8 : 2). Purification by silica gel chromatography afforded β-amino ester **13** (335 mg, 38%) as needle-like crystals. ^{1}H NMR (300 MHz, $CDCl_3$) δ 3.52 (m, 1H), 3.13 (d, J = 8.1 Hz, 1H), 2.46 (m, 1H), 1.60–1.46 (m, 3H), 1.42 (m, 10H), 1.18 (s, 9H), 1.07 (d, J = 7.1 Hz, 3H), 0.91 (t, J = 6.9 Hz, 3H); ^{13}C NMR (75 MHz, $CDCl_3$) δ 173.8, 80.7, 59.0, 56.3, 45.2, 36.6, 28.2, 22.9, 19.4, 13.9, 11.8. HRMS (ESI-TOF) calcd for $C_{15}H_{31}NO_3H^+$ $[M + H]^+$ 306.2103, found 306.2110.

(2*S*,3*R*)-3-Fmoc-amino-2-methylhexanoic acid (14). TFA (5.0 mL) was added to a solution of β-amino ester **13** (224 mg, 0.73 mmol) in anhydrous CH_2Cl_2 (5.0 mL). After 25 hours the reaction mixture was concentrated and residual TFA was removed by co-evaporation with toluene (3 × 10 mL). The resulting residue was dissolved in dioxane (5.0 mL) and HCl in dioxane (4 M, 0.55 mL, 2.2 mmol, 3.0 equiv.) was added. After 1.5 hours the mixture was concentrated. The crude fully deprotected β-amino acid was suspended in water (5.0 mL) at 0 °C and Na_2CO_3 (311 mg, 2.93 mmol, 4.0 equiv.) was added followed by Fmoc-*O*-succinimide (297 mg, 0.88 mmol, 1.2 equiv.) in DMF (3.0 mL). Cooling was removed and DMF (2.0 mL) was added. After 1.5 hours, water (5.0 mL) was added and after additionally 1.5 hours of stirring the reaction mixture was diluted with water (60 mL) and extracted with Et_2O (15 mL). After acidification with concentrated HCl, until pH ≈ 1–2, the aqueous layer was extracted with EtOAc (3 × 75 mL). The combined organic phases were dried ($MgSO_4$), filtered, and concentrated *in vacuo*. Purification of the crude residue by vacuum silica gel chromatography afforded β-amino acid **14** (66 mg, 25%, 3 steps) as a white solid after co-evaporation of residual acetic acid with CH_2Cl_2–toluene (1 : 1, 3 × 10 mL); ^{1}H NMR (300 MHz, DMSO-d_6) δ 12.19 (s, 1H), 7.86 (d, J = 7.4 Hz, 2H), 7.66 (dd, J = 7.3, 2.9 Hz, 2H), 7.38 (t, J = 7.4 Hz, 2H), 7.30 (d, J = 7.4, 2H), 7.05 (d, J = 9.5 Hz, 1H), 4.31 (m, 2H), 4.18 (t, J = 6.7 Hz, 1H), 3.58 (m, 1H),

2.28 (m, 1H), 1.22 (m, 4H), 0.95 (d, $J = 6.9$ Hz, 3H), 0.79 (t, $J = 6.9$ Hz, 3H); ^{13}C NMR (75 MHz, DMSO-d_6) δ 176.2, 156.2, 143.9, 140.8, 127.6, 127.1, 127.0, 125.2 (2C), 120.1, 65.0, 52.4, 46.9, 44.4, 35.0, 18.8, 14.0, 13.7. HRMS (ESI-TOF) calcd for $C_{22}H_{25}NO_4H^+$ $[M + H]^+$ 368.1862, found 368.1863.

(2*S*,3*R*)-Methyl 3-(((benzyloxy)carbonyl)amino)-2-methylhexanoate (15). HCl in dioxane (4 M, 4.7 mL, 18.8 mmol, 30 equiv.) was added to a solution of β-amino ester **13** (190 mg, 0.62 mmol) in MeOH (5.0 mL). After stirring for 22 hours the mixture was concentrated. ^{1}H NMR of the crude residue showed a mixture of the fully deprotected β-amino acid and amine deprotected methyl ester. To ensure full conversion to the methyl ester the crude product was dissolved in MeOH (5.0 mL) under Ar, cooled to 0 °C, and thionyl chloride (70 μL, 0.94 mmol, 1.5 equiv.) was added dropwise. After 10 min the reaction mixture was heated under reflux for 20 hours before additional thionyl chloride (70 μL, 0.94 mmol, 1.5 equiv.) was added. After further 2.5 hours of stirring the mixture was concentrated and redissolved in MeOH (5.0 mL). Thionyl chloride (90 μL, 1.23 mmol, 2.0 equiv.) was added at 0 °C and the mixture stirred for 22 hours at room temperature, before concentration afforded the crude amine. The crude amine was dissolved in sat. aqueous $NaHCO_3$–EtOAc (1 : 1, 6.0 mL) and benzylchloroformate (133 μL, 0.93 mmol, 1.5 equiv.) was added. After 18 hours of vigorous stirring the phases were separated and the aqueous layer was diluted with water (5 mL) and extracted with ethyl acetate (2 × 5 mL). The combined organic phases were washed with aqueous HCl (1 M, 6 mL) and brine (6 mL), dried (Na_2SO_4), filtered, and concentrated *in vacuo*. Purification by vacuum silica gel chromatography afforded the β-amino ester **15** (37%, three steps from **13**). $[\alpha]_D^{20}$ −39° ($CHCl_3$, c 1.0), previously reported $[\alpha]_D^{20}$ −34° ($CHCl_3$, c 1.0);[32] ^{1}H NMR (400 MHz, $CDCl_3$) δ 7.38–7.28 (m, 5H), 5.09 (s, 2H), 4.95 (d, $J = 9.7$ Hz, 1H), 3.93–3.82 (m, 1H), 3.67 (s, 3H), 2.65 (m, 1H), 1.43 (m, 2H), 1.31 (m, 2H), 1.15 (d, $J = 7.2$ Hz, 3H), 1.15 (d, $J = 7.2$ Hz, 3H); ^{13}C NMR (100 MHz, $CDCl_3$) δ 175.0, 156.2, 136.7, 128.6, 128.2 (2C), 66.8, 53.2, 51.9, 44.1, 34.2, 19.6, 13.9, 13.2. The spectral data were in full accordance with those reported in the literature (see ESI, Table S1†).[32]

Linear peptide 16. Polystyrene 2-chlorotrityl-bound Fmoc-D-Val–D-Ala–D-Tyr (140 mg, 0.11 mmol) was added to a fritted syringe and the Fmoc group was removed with piperidine–DMF (1 : 4, 4 mL, 2 × 30 min) and DBU–piperidine–DMF (2 : 2 : 96, 4 mL, 30 min). The resin was then washed with DMF (×3), MeOH (×3), and CH_2Cl_2 (×3). β-Amino acid **14** (43 mg, 0.12 mmol, 1.1 equiv.) in DMF (2.0 mL) was preincubated for 5 min with 2,6-lutidine (37 μL, 0.32 mmol, 3.0 equiv.) and HATU (61 mg, 0.16 mmol, 1.5 equiv.) before addition to the resin and the reaction was allowed to proceed on a rocking table for 17 hours. After washing with DMF (×3), MeOH (×3), and CH_2Cl_2 (×3) the Fmoc group was removed with piperidine–DMF (1 : 4, 4 mL, 2 × 30 min) and DBU–piperidine–DMF (2 : 2 : 96, 4 mL, 30 min). The resin was then washed again and treated with TFA–CH_2Cl_2 (1 : 1, 4 mL) for 30 min followed by washing with CH_2Cl_2 (5 mL). A fresh portion of TFA–CH_2Cl_2 (1 : 1, 4 mL) was added to the resin and after additional 30 min the resin was drained and all the fractions were pooled and concentrated *in vacuo* to provide the linear peptide as an oily residue. Trituration with diethyl ether afforded the TFA salt of the linear peptide **16** (53 mg, 81% from 2-chlorotrityl chloride resin, based on theoretical loading of resin) as a white solid. UPLC-MS, $t_R = 0.84$ min, calcd for $C_{24}H_{38}N_4O_6H^+$ $[M + H]^+$ 479.3, found 479.3; ^{1}H NMR (400 MHz, MeOD) δ 7.04 (d, $J = 8.2$ Hz, 2H), 6.69 (d, $J = 8.2$ Hz, 2H), 4.58 (m, 1H), 4.38 (m, 1H), 4.15 (d, $J = 7.1$ Hz, 1H), 3.38 (m, 1H), 3.07 (dd, $J = 14.0$, 5.3 Hz, 1H), 2.92 (dd, $J = 14.0$, 7.8 Hz, 1H), 2.79 (m, 1H), 2.05 (octet, $J = 6.9$ Hz, 1H), 1.60 (q, J =7.8 Hz, 2H), 1.54–1.39 (m, 2H), 1.33 (d, $J = 7.1$ Hz, 3H), 1.21 (d, $J = 7.2$ Hz, 3H), 0.99 (t, $J = 7.3$ Hz, 3H), 0.93 (d, $J = 6.8$ Hz, 6H).

Cyclic peptide 9. Linear peptide **16** (50 mg, 0.084 mmol) was dissolved in DMF (200 mL ≈ 0.4 mM) and iPr_2NEt (73 μL, 0.42 mmol, 5.0 equiv.) and HATU (48 mg, 0.13 mmol, 1.5 equiv.) were added. After stirring for 19 hours the reaction mixture was concentrated *in vacuo*. The residue was taken up in CH_2Cl_2 (80 mL) and washed with aqueous HCl (1 M, 2 × 15 mL) and the aqueous phase was re-extracted with CH_2Cl_2 (50 mL). The combined organics were washed with brine (25 mL), dried ($MgSO_4$), filtered, and concentrated *in vacuo*. The resulting residue was dissolved in DMF (2.5 mL) and purified by preparative HPLC on a [250 mm × 20 mm, C_{18} Phenomenex Luna column (5 μm, 100 Å)] using an Agilent 1260 LC system to afford the cyclic peptide **9** (2.7 mg, 7%) as a white solid. A gradient with eluent III (95 : 5 : 0.1, water–MeCN–TFA) and eluent IV (0.1% TFA in acetonitrile) rising linearly from 0% to 95% of eluent IV during $t = 5$–45 min was applied at a flow rate of 20 mL min^{-1}. Two conformations are observed in the ^{1}H NMR spectrum. The conformations are present in an 88 : 12 ratio. Characterization is given for the major conformation. ^{1}H NMR (500 MHz, DMSO-d_6) δ 9.19 (br s, 1H), 7.67 (d, $J = 8.8$ Hz, 1H), 7.55 (d, $J = 9.0$ Hz, 1H), 7.46 (d, $J = 8.4$ Hz, 1H), 6.96 (m, 3H), 6.63 (d, $J = 8.4$ Hz, 2H), 4.14 (p, $J = 7.3$ Hz, 1H), 4.07 (p, $J = 8.8$ Hz, 1H), 3.99 (m, 1H), 3.67 (t, $J = 9.4$ Hz 1H), 2.89 (dd, $J = 13.7$, 7.2 Hz, 1H), 2.81 (dd, $J = 13.7$, 9.0 Hz, 1H), 2.54 (m, 1H), 2.16 (m, 1H), 1.64 (m, 1H), 1.36 (m, 1H), 1.25–1.15 (m, 8H), 0.91–0.77 (m, 9H); HRMS (ESI-TOF) calcd for $C_{24}H_{36}N_4O_5H^+$ $[M + H]^+$ 461.2719, found 461.2754; HPLC gradient B, $t_R = 11.14$ min (>95%).

Biochemical profiling

***In vitro* histone deacetylase inhibition assays.** For assaying, peptides were reconstituted in DMSO to give 5–10 mM stock solutions, the accurate concentrations of which were determined by UV using the extinction coefficient for tyrosine at 280 nm; $\varepsilon = 1280$ M^{-1} × cm^{-1}. Inhibition of recombinant human HDACs in dose–response experiments with internal controls was measured in black low binding Corning half-area 96-well microtiter plates. The appropriate dilution of inhibitor (5 μL of 5× the desired final concentration, prepared from 5–10 mM DMSO stock solutions) was added to each well followed by substrate in HDAC assay buffer (10 μL). Ac–Leu–Gly–Lys (Ac)–AMC was used at a final concentration of 20 μM for HDAC1, 2, 3, 6, and 11. Ac–Leu–Gly–Lys (Tfa)–AMC was used at a final concentration of 20 μM for HDAC4, 120 μM for HDAC5, 40 μM for HDAC7 and 200 μM for HDAC8, and 80 μM for HDAC9. Ac–Arg–His–Lys (Ac)–Lys (Ac)–AMC was used at a final

concentration of 5 μM for HDAC10. Finally, a freshly prepared solution of the appropriate HDAC (10 μL) was added and the plate (containing a final volume of 25 μL in each well) was incubated at 37 °C for 30 min. The final concentrations of enzyme was as follows: HDAC1: 1 ng μL^{-1}, HDAC2: 0.5 ng μL^{-1}, HDAC3-NCoR2: 0.09 ng μL^{-1}, HDAC4: 0.04 ng μL^{-1}, HDAC5: 0.2 ng μL^{-1}, HDAC6: 2.4 ng μL^{-1}, HDAC7: 0.04 ng μL^{-1}, HDAC8: 0.2 ng μL^{-1}, HDAC9: 0.8 ng μL^{-1}, HDAC10: 4 ng μL^{-1}, HDAC11: 10 ng μL^{-1}. Then trypsin (25 μL, 0.4 mg mL^{-1}) was added and the assay development was allowed to proceed for 15–30 min at room temperature, before the plate was read using a Perkin Elmer Enspire plate reader with excitation at 360 nm and detecting emission at 460 nm. Each assay was performed in duplicate and repeated at least twice. The data were analyzed by non-linear regression using GraphPad Prism to afford IC_{50} values from the dose–response experiments, and K_i values were determined from the Cheng–Prusoff equation, $K_i = IC_{50}/(1 + [S]/K_m)$, assuming a standard fast-on–fast-off mechanism of inhibition. The applied K_m values were previously reported for HDACs 1–3,[35] HDAC10,[29] and HDAC11.[36]

Continuous assay protocol. The continuous assays of HDAC3-NCoR2 inhibition were performed in 96-well, white, medium binding, half-area microtiter plates (Greiner Bio One). The 2- or 3-fold dilution series of inhibitors were prepared as described above. HDAC assay buffer (10 μL) containing substrate Ac–Leu–Gly–Lys (Ac)–AMC (100 μM; final concentration 20 μM) and HDAC assay buffer (10 μL) containing trypsin (12.5 ng μL^{-1}; final concentration 2.5 ng μL^{-1}) was added to each well, followed by the appropriate dilution of inhibitor (20 μL of 2.5× the desired final concentration). Finally, a solution of HDAC3-NCoR2 (10 μL, 0.2 ng μL^{-1} = 2.5 nM; final concentration 0.04 ng μL^{-1} = 0.5 nM) was added, and fluorescence readings were recorded every 30 seconds for 45 min at 25 °C using a Perkin Elmer Enspire plate reader with excitation at 360 nm and detecting emission at 460 nm. Each assay was performed twice in duplicate. The rate constants (v) were determined by linear regression analysis using GraphPad Prism. K_i values were then determined by non-linear fitting to the following equation, $v_i/v_0 = (1 + [I]/(K_i(1 + [S]/K_m)))^{-1}$.

***In vitro* cell proliferation assay.** Cell proliferation was assessed using the MTT cell growth kit (Millipore, Billerica, MA, USA). EB-3 cells (ATCC, Manassas, VA, USA) were seeded in 96-well flat-bottom cell culture plates (Nunc, Thermo Fischer Scientific, Roskilde, Denmark) with a density of 2×10^4 cells in 90 μL culture media composed of RPMI-1640 (ATCC, Manassas, VA, USA) supplemented with 10% fetal calf serum (FCS) (Sera Scandia, Hellerup, Denmark) and 1% penicillin/streptomycin (Gibco, Invitrogen, Taastrup, Denmark). After cultivation overnight at 37 °C in humid 5% CO_2 atmosphere, 10 μL of culture medium containing appropriate concentrations of the five compounds or the vehicle (DMSO) as control were added. The 2-fold dilution series were prepared from DMSO stock solutions (5 mM for azumamide C and 10 mM for the remaining compounds) to give final assay concentrations starting from 50 μM for azumamide C, SAHA, and apicidin while 100 μM was applied for azumamide B and compound **9**. After incubation for 3 days, MTT solution was freshly prepared by dissolving 3-(4,5-dimethylthiazol-2-yl)-2,5-diphenyltetrazolium bromide (MTT, 50 mg) in PBS (10 mL, both supplied in the MTT assay kit) and 10 μL of this solution was added to each well. The cells were incubated for another 4 h at 37 °C in humid 5% CO_2 atmosphere for development to take place. The purple formazan crystals produced were dissolved by addition of isopropyl alcohol (100 μL per well) containing HCl (0.04 M), and the absorbance was measured at 570 nm with background subtraction at 630 nm on a Tecan Sunrise ELISA plate reader (Tecan, Switzerland). All assays were performed three times in duplicate.

Acknowledgements

We thank Ms Tina Gustafsson (DTU Chemistry) and Esin Güven (KBIG, SSI) for technical assistance. We gratefully acknowledge financial support from the Danish Independent Research Council–Technology and Production Sciences (Sapere Aude Grant no. 12-132328; A.S.M.), the Danish Independent Research Council–Natural Sciences (Steno Grant no. 10-080907; C.A.O.), the Carlsberg Foundation (C.A.O.), and the Lundbeck Foundation (Young Group Leader Fellowship to C.A.O.).

References

1 I. V. Gregoretti, Y. M. Lee and H. V. Goodson, *J. Mol. Biol.*, 2004, **338**, 17–31.
2 G. Blander and L. Guarente, *Annu. Rev. Biochem.*, 2004, **73**, 417–435.
3 M. D. Hirschey, *Cell Metab.*, 2011, **14**, 718–719.
4 C. A. Olsen, *Angew. Chem., Int. Ed.*, 2012, **51**, 3755–3756.
5 C. A. Olsen, *ChemMedChem*, 2014, **9**, 434–437.
6 C. H. Arrowsmith, C. Bountra, P. V. Fish, K. Lee and M. Schapira, *Nat. Rev. Drug Discovery*, 2012, **11**, 384–400.
7 M. C. Haigis and D. A. Sinclair, *Annu. Rev. Pathol.: Mech. Dis.*, 2010, **5**, 253–295.
8 M. Haberland, R. L. Montgomery and E. N. Olson, *Nat. Rev. Genet.*, 2009, **10**, 32–42.
9 A. G. Kazantsev and L. M. Thompson, *Nat. Rev. Drug Discovery*, 2008, **7**, 854–868.
10 P. A. Marks and R. Breslow, *Nat. Biotechnol.*, 2007, **25**, 84–90.
11 H. M. Prince and M. Dickinson, *Clin. Cancer Res.*, 2012, **18**, 3509–3515.
12 A. C. West and R. W. Johnstone, *J. Clin. Invest.*, 2014, **124**, 30–39.
13 H. Rajak, A. Singh, P. K. Dewangan, V. Patel, D. K. Jain, S. K. Tiwari, R. Veerasamy and P. C. Sharma, *Curr. Med. Chem.*, 2013, **20**, 1887–1903.
14 F. F. Wagner, M. Weïwer, M. C. Lewis and E. B. Holson, *Neurotherapeutics*, 2013, **10**, 589–604.
15 P. Bertrand, *Eur. J. Med. Chem.*, 2010, **45**, 2095–2116.
16 S. J. Darkin-Rattray, A. M. Gurnett, R. W. Myers, P. M. Dulski, T. M. Crumley, J. J. Allocco, C. Cannova, P. T. Meinke, S. L. Colletti, M. A. Bednarek, S. B. Singh, M. A. Goetz, A. W. Dombrowski, J. D. Polishook and D. M. Schmatz, *Proc. Natl. Acad. Sci. U. S. A.*, 1996, **93**, 13143–13147.
17 P. T. Meinke, S. L. Colletti, G. Doss, R. W. Myers, A. M. Gurnett, P. M. Dulski, S. J. Darkin-Rattray,

J. J. Allocco, S. Galuska, D. M. Schmatz, M. J. Wyvratt and M. H. Fisher, *J. Med. Chem.*, 2000, **43**, 4919–4922.
18 S. L. Colletti, R. W. Myers, S. J. Darkin-Rattray, A. M. Gurnett, P. M. Dulski, S. Galuska, J. J. Allocco, M. B. Ayer, C. Li, J. Lim, T. M. Crumley, C. Cannova, D. M. Schmatz, M. J. Wyvratt, M. H. Fisher and P. T. Meinke, *Bioorg. Med. Chem. Lett.*, 2001, **11**, 107–111.
19 S. L. Colletti, R. W. Myers, S. J. Darkin-Rattray, A. M. Gurnett, P. M. Dulski, S. Galuska, J. J. Allocco, M. B. Ayer, C. Li, J. Lim, T. M. Crumley, C. Cannova, D. M. Schmatz, M. J. Wyvratt, M. H. Fisher and P. T. Meinke, *Bioorg. Med. Chem. Lett.*, 2001, **11**, 113–117.
20 W. S. Horne, C. A. Olsen, J. M. Beierle, A. Montero and M. R. Ghadiri, *Angew. Chem., Int. Ed.*, 2009, **48**, 4718–4724.
21 A. Montero, J. M. Beierle, C. A. Olsen and M. R. Ghadiri, *J. Am. Chem. Soc.*, 2009, **131**, 3033–3041.
22 C. A. Olsen and M. R. Ghadiri, *J. Med. Chem.*, 2009, **52**, 7836–7846.
23 C. A. Olsen, A. Montero, L. J. Leman and M. R. Ghadiri, *ACS Med. Chem. Lett.*, 2012, **3**, 749–753.
24 C. J. Vickers, C. A. Olsen, L. J. Leman and M. R. Ghadiri, *ACS Med. Chem. Lett.*, 2012, **3**, 505–508.
25 I. Izzo, N. Maulucci, G. Bifulco and F. De Riccardis, *Angew. Chem., Int. Ed.*, 2006, **45**, 7557–7560.
26 Y. Nakao, S. Yoshida, S. Matsunaga, N. Shindoh, Y. Terada, K. Nagai, J. K. Yamashita, A. Ganesan, R. W. M. van Soest and N. Fusetani, *Angew. Chem., Int. Ed.*, 2006, **45**, 7553–7557.
27 N. Maulucci, M. G. Chini, S. D. Micco, I. Izzo, E. Cafaro, A. Russo, P. Gallinari, C. Paolini, M. C. Nardi, A. Casapullo, R. Riccio, G. Bifulco and F. De Riccardis, *J. Am. Chem. Soc.*, 2007, **129**, 3007–3012.
28 D. Wang, P. Helquist and O. Wiest, *J. Org. Chem.*, 2007, **72**, 5446–5449.
29 J. S. Villadsen, H. M. Stephansen, A. R. Maolanon, P. Harris and C. A. Olsen, *J. Med. Chem.*, 2013, **56**, 6512–6520.
30 T. P. Tang and J. A. Ellman, *J. Org. Chem.*, 2002, **67**, 7819–7832.
31 M. T. Robak, M. A. Herbage and J. A. Ellman, *Chem. Rev.*, 2010, **110**, 3600–3740.
32 J. E. Wilson, A. D. Casarez and D. W. MacMillan, *J. Am. Chem. Soc.*, 2009, **131**, 11332–11334.
33 C. J. White and A. K. Yudin, *Nat. Chem.*, 2011, **3**, 509–524.
34 Y. Cheng and W. H. Prusoff, *Biochem. Pharmacol.*, 1973, **22**, 3099–3108.
35 J. E. Bradner, N. West, M. L. Grachan, E. F. Greenberg, S. J. Haggarty, T. Warnow and R. Mazitschek, *Nat. Chem. Biol.*, 2010, **6**, 238–243.
36 A. S. Madsen and C. A. Olsen, *Angew. Chem., Int. Ed.*, 2012, **51**, 9083–9087.
37 P. J. Watson, L. Fairall, G. M. Santos and J. W. Schwabe, *Nature*, 2012, **481**, 335–340.
38 M. Bantscheff, C. Hopf, M. M. Savitski, A. Dittmann, P. Grandi, A. M. Michon, J. Schlegl, Y. Abraham, I. Becher, G. Bergamini, M. Boesche, M. Delling, B. Dümpelfeld, D. Eberhard, C. Huthmacher, T. Mathieson, D. Poeckel, V. Reader, K. Strunk, G. Sweetman, U. Kruse, G. Neubauer, N. G. Ramsden and G. Drewes, *Nat. Biotechnol.*, 2011, **29**, 255–265.
39 C. J. Chou, D. Herman and J. M. Gottesfeld, *J. Biol. Chem.*, 2008, **283**, 35402–35409.
40 J. A. Richter-Larrea, E. F. Robles, V. Fresquet, E. Beltran, A. J. Rullan, X. Agirre, M. J. Calasanz, C. Panizo, J. A. Richter, J. M. Hernandez, J. Roman-Gomez, F. Prosper and J. A. Martinez-Climent, *Blood*, 2010, **116**, 2531–2542.
41 F. A. Davis, M. B. Nolt, Y. Wu, K. R. Prasad, D. Li, B. Yang, K. Bowen, S. H. Lee and J. H. Eardley, *J. Org. Chem.*, 2005, **70**, 2184–2190.

Electronic Supplementary Information

An azumamide C analogue without the zinc-binding functionality

Jesper S. Villadsen,[a] Betül Kitir,[ab] Kathrine Wich,[b] Tina Friis,[c] Andreas S. Madsen,[ab] and Christian A. Olsen*[ab]

General Experimental

Materials and methods. All chemicals and solvents were analytical grade and used without further purification. Vacuum liquid chromatography (VLC) was performed on silica gel 60 (particle size 0.015−0.040μm). UPLC−MS analyses were performed on a Waters Acquity ultra high-performance liquid chromatography system. A gradient with eluent I (0.1% HCOOH in water) and eluent II (0.1% HCOOH in acetonitrile) rising linearly from 0% to 95% of II during t = 0.00–2.50 min was applied at a flow rate of 1 mL/min. Analytical HPLC was performed on a [150 mm × 4.6 mm, C_{18} Phenomenex Luna column (3 μm)] using an Agilent 1100 LC system equipped with a UV detector. A gradient, B, with eluent III (95:5:0.1, water−MeCN−TFA) and eluent IV (0.1% TFA in acetonitrile) rising linearly from 0% to 95% of IV during t = 2−20 min was applied at a flow rate of 1 mL/min. Preparative reversed-phase HPLC was performed on a [250 mm × 20 mm, C_{18} Phenomenex Luna column (5 μm, 100 Å)] using an Agilent 1260 LC system equipped with a diode array UV detector and an evaporative light scattering detector (ELSD). A gradient C with eluent III (95:5:0.1, water−MeCN−TFA) and eluent IV (0.1% TFA in acetonitrile) rising linearly from 0% to 95% of IV during t = 5−45 min was applied at a flow rate of 20 mL/min. 1D and 2D NMR spectra were recorded on a Varian INOVA 500 MHz instrument, a Bruker Ascend 400 MHz or a Varian Mercury 300 instrument. All spectra were recorded at 298 K. For the Varian INOVA 500 MHz instrument and the Varian Mercury 300 instrument 1D NMR spectra were recorded at 499.9 MHz and 300 MHz for 1H and 100 MHz and 75 MHz for 13C, respectively. The correlation spectroscopy (COSY) spectra were recorded with a relaxation delay of 1.5 sec before each scan, a spectral width of 6k × 6k, collecting 8 FIDs and 1k × 512 data points. Heteronuclear single quantum coherence (HSQC) spectra were recorded with a relaxation delay of 1.5 sec before each scan, a spectral width of 6k × 25k, collecting 16 FIDs and 1k × 128 data points. Heteronuclear 2-bond correlation (H2BC) spectra were recorded with a relaxation delay of 1.5 sec before each scan, a spectral width of 4k × 35k, collecting 16 FIDs at 295 K and 1k × 256 datapoints. Heteronuclear multiple-bond correlation (HMBC) spectra were recorded with a relaxation delay of 1.5 sec before each scan, a spectral width of 6k × 35 k, collecting 32 FIDs and 1k × 256 datapoints. Finally, on the Bruker Ascend 400 MHz the 1D NMR spectra were recorded at 400 MHz for 1H and 100 MHz for 13C. The correlation spectroscopy (COSY) spectra were recorded with a relaxation delay of 1.5 sec before each scan, a spectral width of 3k × 3k, collecting 4 FIDs and 1k × 128 data points. The heteronuclear single quantum coherence (HSQC) spectra were recorded with a relaxation delay of 1.5 sec before each scan, a spectral width of 4800 × 16600, collecting 4 FIDs and 1k × 256 datapoints. Chemical shifts are reported in ppm relative to deuterated solvent peaks as internal standards (δH, DMSO-d_6 2.50 ppm; δC, DMSO-d_6 39.52 ppm, δH, $CDCl_3$ 7.26 ppm; δC, $CDCl_3$ 77.16 ppm). Coupling constants (J) are given in hertz (Hz). Multiplicities of ^{1}H NMR signals are reported as follows: s, singlet; d, doublet; t, triplet; q, quartet; m, multiplet.

Assay materials. HDAC1 (Purity ≥62% by SDS-PAGE according to the supplier), HDAC2 (Full length, purity ≥94% by SDS-PAGE according to the supplier), HDAC3-NCoR2 complex (Purity ≥80% by SDS-PAGE according to supplier, HDAC4 (Purity ≥60% by SDS-PAGE according to the supplier) and HDAC 5 (Full length, purity ≥90% by SDS-PAGE according to the supplier), HDAC8 (Purity ≥90% by SDS-PAGE according to the supplier), HDAC9 (Full length, purity ≥76% by SDS-PAGE according to the supplier) and HDAC10 (Purity ≥21% by SDS-PAGE according to the supplier) were purchased from BPS Bioscience (San Diego, CA 92121). HDAC 7 (Purity ≥90% by SDS-PAGE according to the supplier) was purchased from Millipore (Temecula, CA 92590). HDAC6 (Purity ≥85% by SDS-PAGE according to the supplier) and HDAC11 (Purity ≥50% by SDS-PAGE according to the supplier) were purchased from Enzo Life Sciences (Postfach, Switzerland). The HDAC assay buffer (50 mM tris/Cl, pH 8.0, 137 mM NaCl, 2.7 mM KCl, 1 mM $MgCl_2$) was added bovine serum albumin (0.5 mg/mL). Trypsin (10,000 units/mg, TPCK treated from bovine pancreas) was from Sigma Aldrich (Steinheim, Germany). All peptides were purified to homogeneity (>95% purity by $HPLC_{230nm}$ using reversed-phase preparative HPLC), and the white fluffy materials obtained by lyophilization were kept at –20 °C.

Table S1. Comparison of ^{1}H and ^{13}C NMR data for reference and compound 15

Position	^{1}H MacMillan[a]	^{13}C MacMillan	^{1}H Compound **15**	^{13}C Compd. **15**
1		174.9		175.0
2	2.71–2.62 (m, 1H)	43.9	2.65 (m, 1H)	44.1
3	3.94–3.84 (m, 1H)	53.0	3.93–3.82 (m, 1H)	53.2
4	1.50–1.38 (m, 2H)	34.0	1.43 (m, 2H)	34.2
5	1.38–1.25 (m, 2H)	19.4	1.31 (m, 2H)	19.6
6	0.92 (bt, *J* = 6.6 Hz, 3H)	13.8	1.15 (d, *J* = 7.2 Hz, 3H)	13.9
OMe	3.58 (s, 3H)	51.8	3.67 (s, 3H)	51.9
α-Me	1.17 (d, *J* = 7.2 Hz, 3H)	13.1	1.15 (d, *J* = 7.2 Hz, 3H)	13.2
Ar	7.41–7.30 (m, 5H)	136.5; 128.5; 128.1×2;	7.38 –7.28 (m, 5H)	136.7; 128.6; 128.2×2;
$PhCH_2$	5.10 (s, 2H)	66.7	5.09 (s, 2H)	66.8
NH	4.93 (d, *J* = 9.5 Hz, 1H)		4.95 (d, *J* = 9.7 Hz, 1H)	
Carbamate		156.0		156.2

[a] Ref 32, J. E. Wilson, A. D. Casarez and D. W. MacMillan, *J. Am. Chem. Soc*., 2009, **131**, 11332-11334.

Figure S1. Single-dose HDAC inhibition experiments.[a]

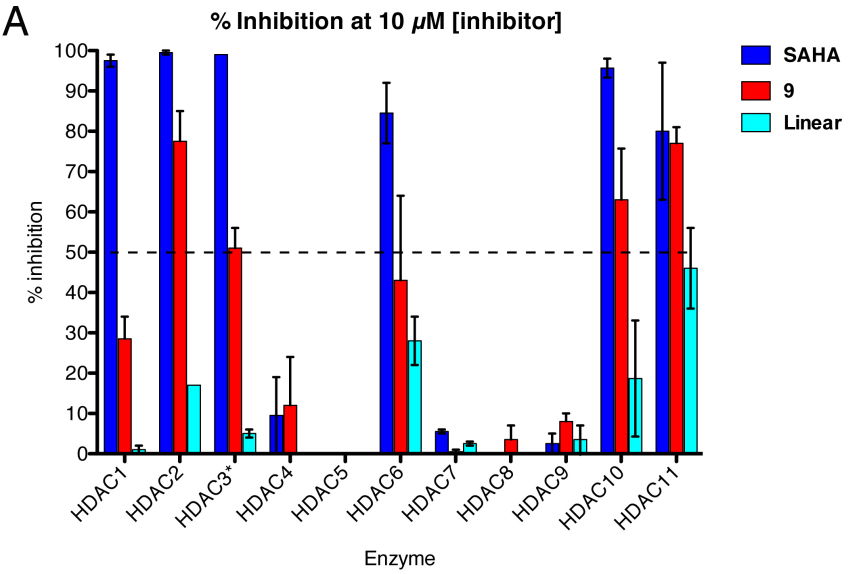

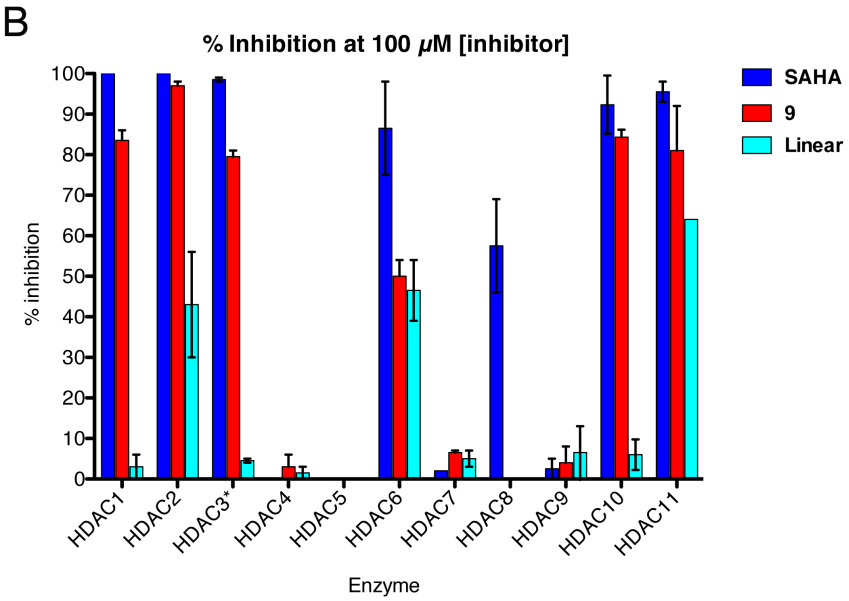

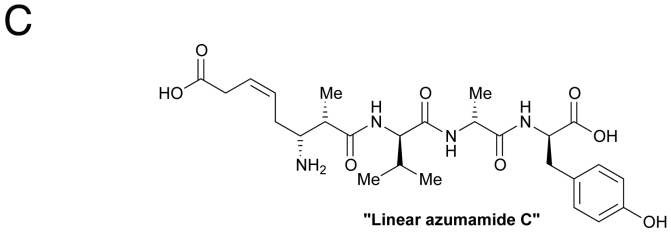

[a]With SAHA (vorinostat) as control compound, we tested the ability of compound **9** as well as the shown linear azumamide C analogue (**C**) to inhibit all the zinc-dependent recombinant human HDAC enzymes at 10 μM (**A**) and 100 μM concentrations (**B**), respectively. *HDAC3 was applied as a complex with NCoR2.

Figure S2. Dose-response HDAC inhibition experiments.[a]

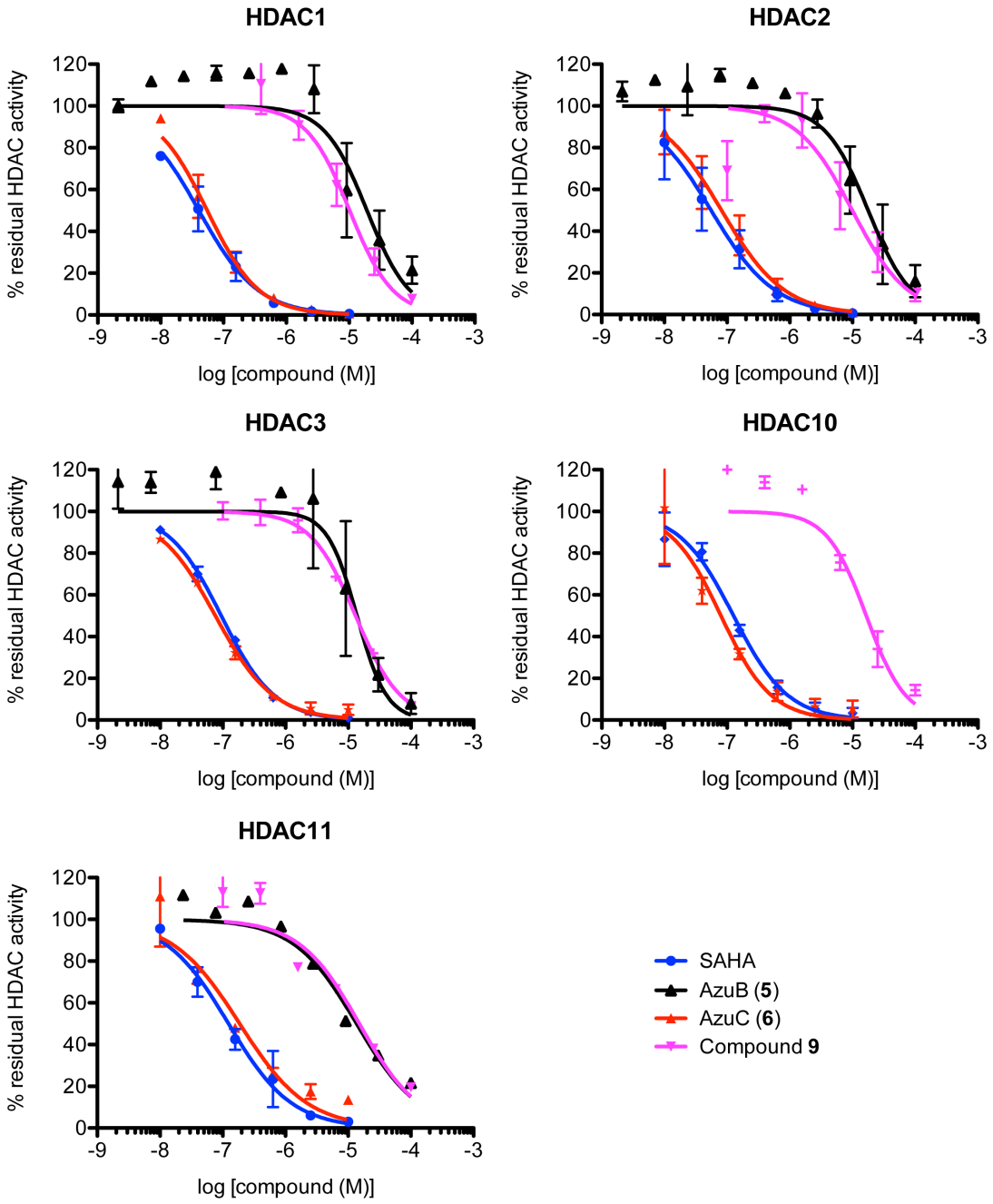

[a]With SAHA (vorinostat) as internal control compound in all assay plates, we performed dose-response experiments in at least two individual assays performed in duplicate. Data for Azumamide B are taken from a previous publication (ref 29, J. S. Villadsen, H. M. Stephansen, A. R. Maolanon, P. Harris, and C. A. Olsen, *J. Med. Chem.*, 2013, **56**, 6512-6520) Data were analyzed and plotted using the GraphPad Prism software. *HDAC3 was applied as a complex with NCoR2.

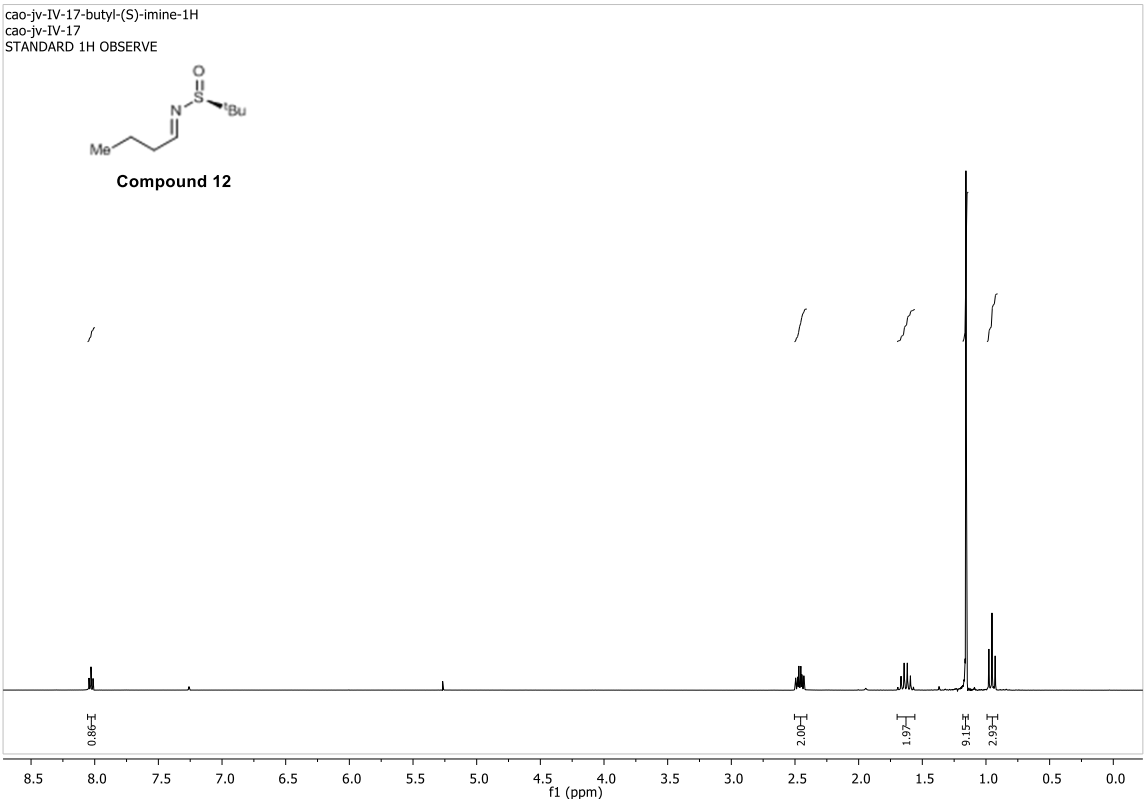
cao-jv-IV-17-butyl-(S)-imine-1H
cao-jv-IV-17
STANDARD 1H OBSERVE
Me
tBu
Compound 12
0.80
2.00
1.97
9.15
2.93
f1 (ppm)

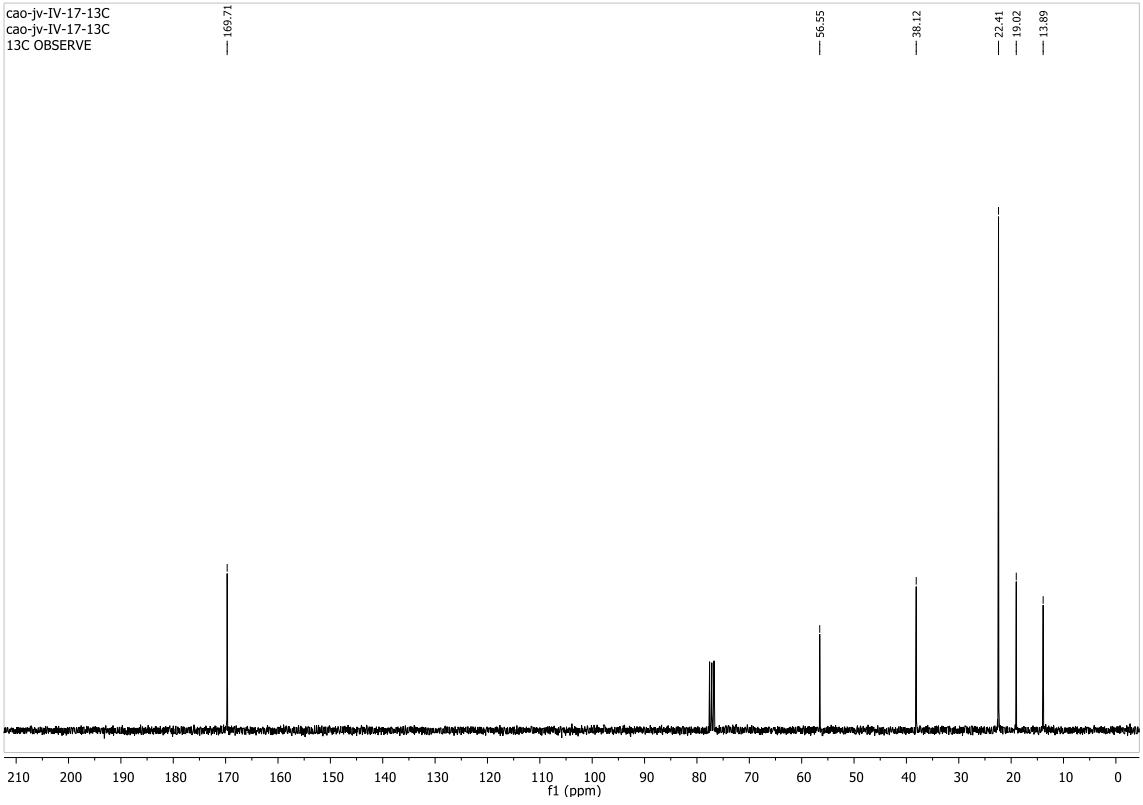
cao-jv-IV-17-13C
cao-jv-IV-17-13C
13C OBSERVE
169.71
56.55
38.12
22.41
19.02
13.89
f1 (ppm)

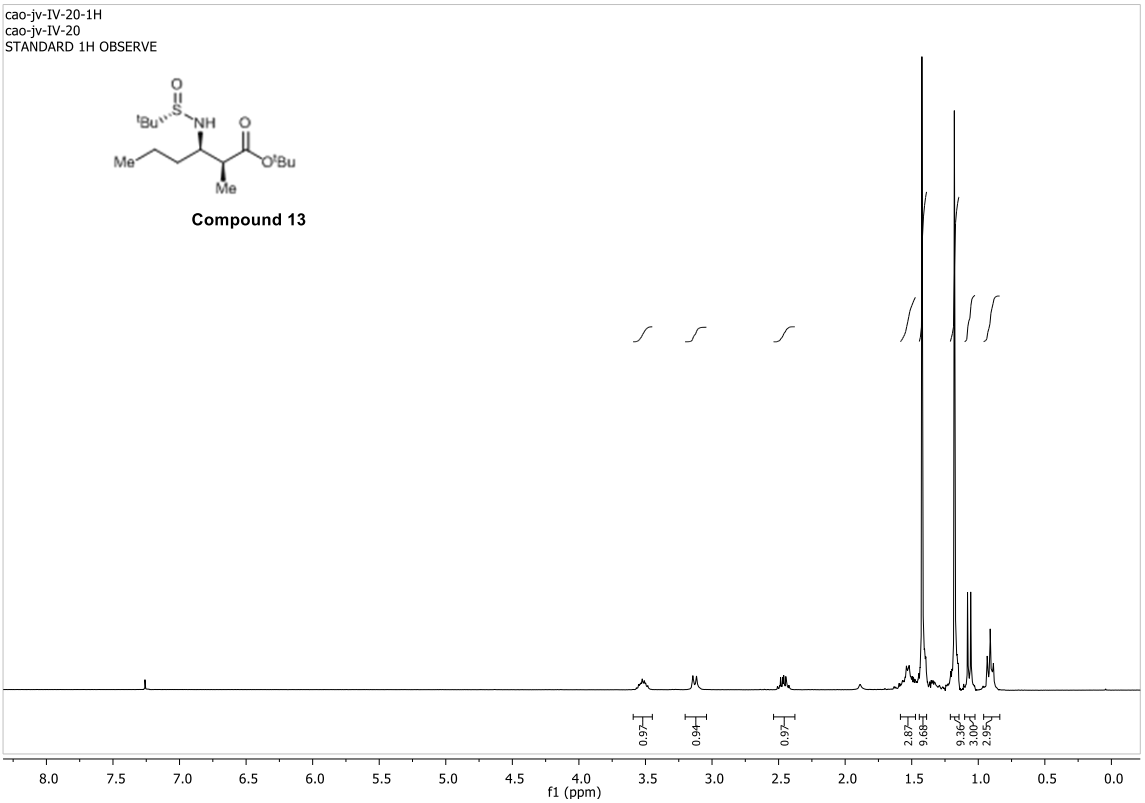
cao-jv-IV-20-1H
cao-jv-IV-20
STANDARD 1H OBSERVE
Compound 13
0.97
0.94
0.97
2.87
9.68
9.36
3.00
2.95
f1 (ppm)

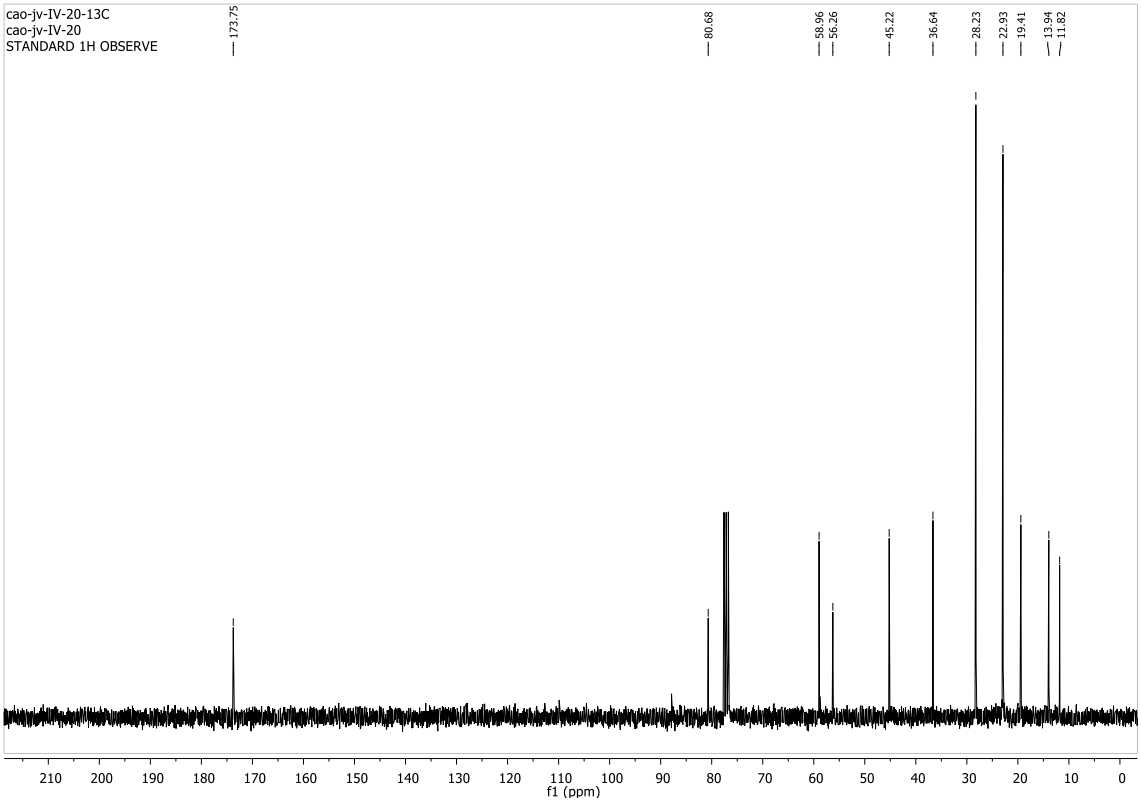
cao-jv-IV-20-13C
cao-jv-IV-20
STANDARD 1H OBSERVE
173.75
80.68
58.96
56.26
45.22
36.64
28.23
22.93
19.41
13.94
11.82
f1 (ppm)

cao-jv-IV-80-1H_1
cao-jv-IV-80
STANDARD 1H OBSERVE

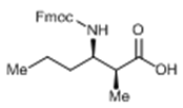

Compound 14

cao-jv-IV-80-13C-5000
cao-jv-IV-80
13C OBSERVE

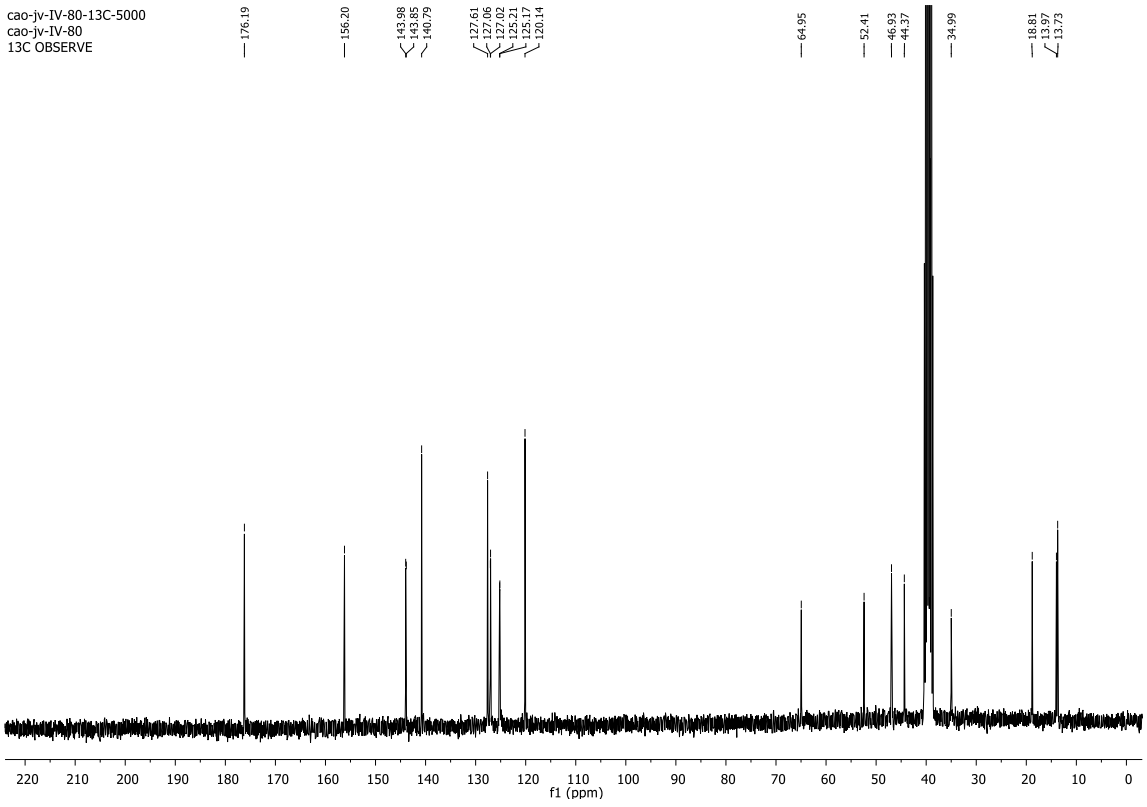

CAO_JV_V-56pure
CAO_JV_V-56pure
1H, 201113, CDCl3

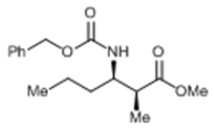

Compound 15

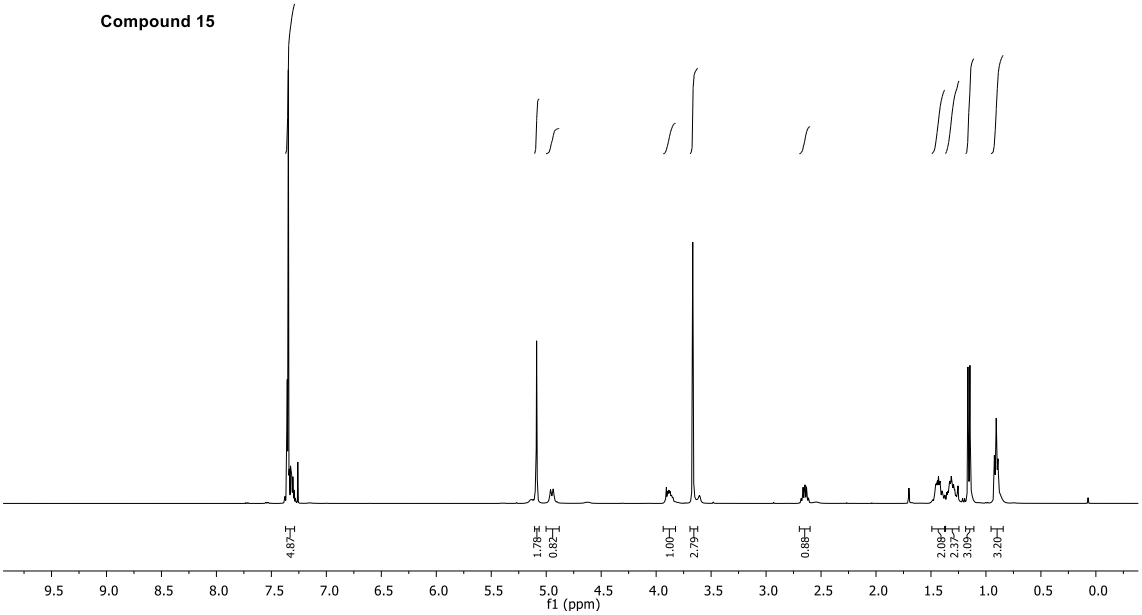

CAO_JV_V-56pure
CAO_JV_V-56pure
13C, 201113, CDCl3

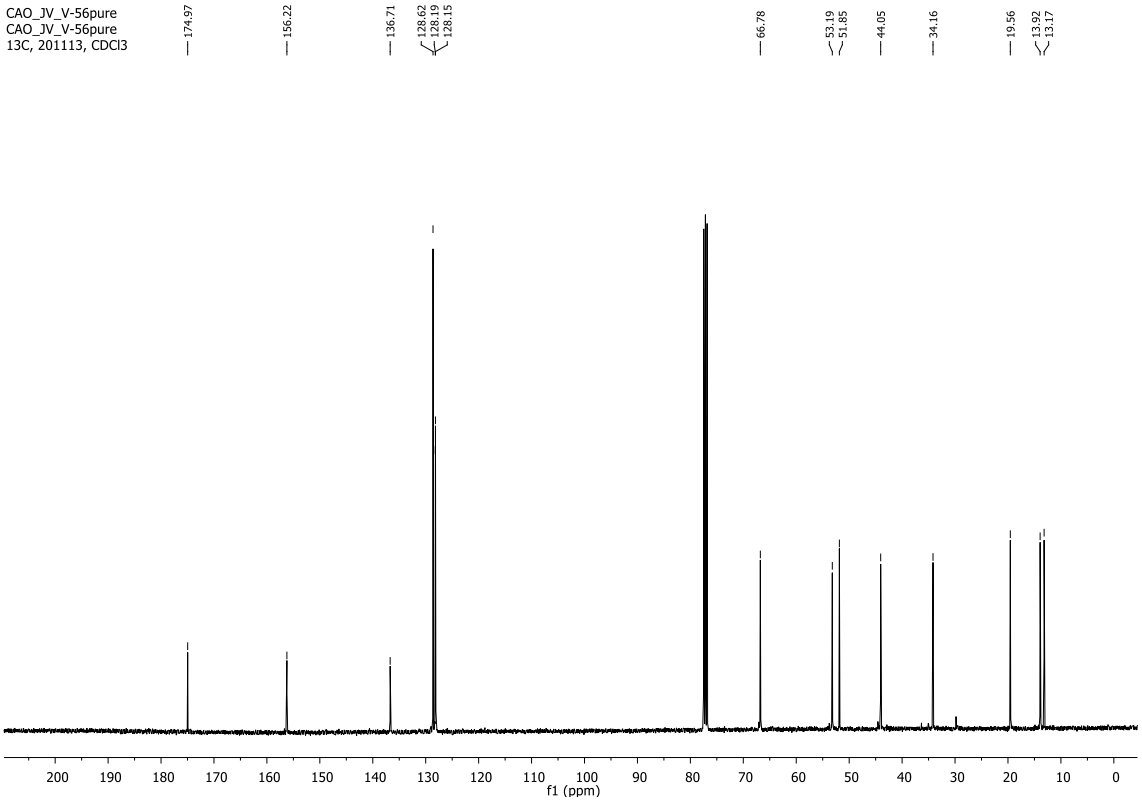

CAO_JV_V-20solid
cao-jv-V-20-solid, 1H, 128 scans, 130613, MeOH

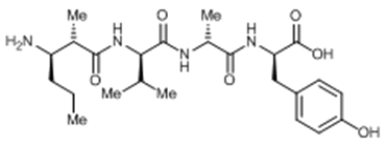

Compound 16

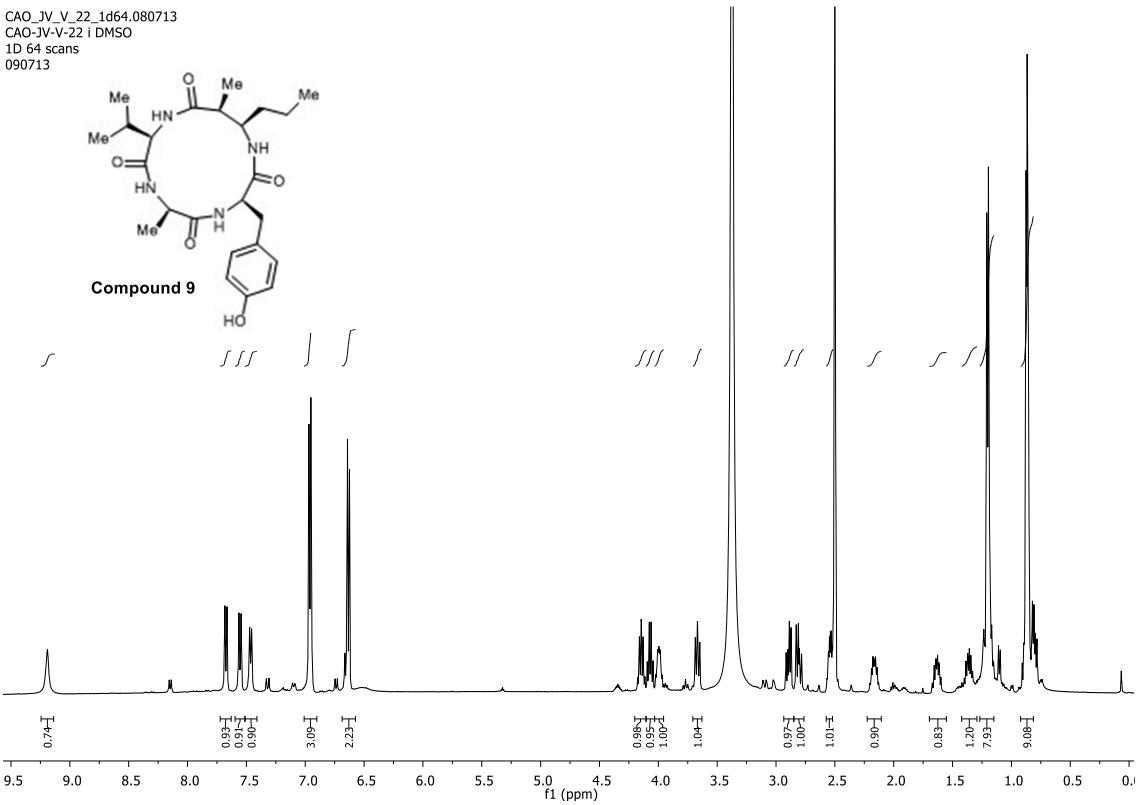
CAO_JV_V_22_1d64.080713
CAO-JV-V-22 i DMSO
1D 64 scans
090713
Compound 9
f1 (ppm)